https://doi.org/10.48048/tis.2022.5765

Flooded Lead Acid Battery SOC Estimation for Energy Conscious LVDC Building: Warm and Humid Climate

Rani Chacko[*], Adarsh Thevarkunnel, Lakaparampil Zachariah Varghese and Jaimol Thomas

Amal Jyothi College of Engineering, APJ Abdul Kalam Technological University, Kerala, India

([*]Corresponding author's e-mail: chacko.rani@gmail.com)

Received: 30 November 2020, Revised: 1 June 2021, Accepted: 8 June 2021

Abstract

Microgrids make it easier to integrate Renewable Energy Sources (RESs) and Energy-Storage Systems (ESSs) at the consumer level, with the intent of enhancing power quality, reliability, and efficiency. This microgrid concept at the nano grid level is championed by a low voltage DC (LVDC) grid, facilitating the direct integration of several distributed generators, storage and loads that are almost DC source/load. Since the State of Charge (SOC) of the battery is an essential parameter for building energy management systems, careful monitoring of SOC is essential. The SOC of a battery directly reflects its performance; thus, straightforward, reasonably accurate, and timely estimation of SOC protects against overcharging or discharging issues, with fewer processor requirements and computations. A novel SOC estimation method is proposed based on the literature assessment of different existing SOC estimation methods. In regions with a tropical climate, the temperature range over the year is small, and the sunshine is relatively intense and fairly even throughout the year. Also, for all practical purposes, it is a fact that the model that takes inputs at the point of use gives accurate results. Considering the 2 facts mentioned above, the current model uses a less complicated algorithm, within acceptable accuracy for the purpose and relatively user-friendly.

Keywords: State of Charge (SOC), Battery thevenin model, Battery internal characteristics, Battery Energy Storage System (BESS), Lead acid battery, Home Energy Management System (HEMS)

Introduction

The current energy sector, which relies immensely on fossil fuels, is heading towards an unsustainable model due to various factors like demand-supply gaps, high carbon footprint, and exponential depletion. Hence great attention is being drawn towards green and renewable energy sources like solar, wind, fuel cell, biomass as an alternative [1]. As these natural energy sources have an unpredictable nature, to use them consistently and reliably, the energy generation from these sources should be coupled with an adequate storage system [2,3]. Today, almost all the existing renewable energy sources like solar photovoltaic, wind generators and fuel cells generate output power as DC or are converted to DC before integrating into the AC grid system. The end-use equipment, especially in a typical residential or commercial building, almost all the connected loads like LED lamps, BLDC fans, mobile and laptop chargers, and inverter setups have internal DC consumption. DC nanogrid should be used to link these DC loads directly to the source to prevent numerous AC-DC and DC-AC conversions. DC has been the most used source of stored energy with the recent developments in battery technology. Together with a dramatic decline in the cost of DC equipment, this extraordinary integration of advances in technology is occurring [4]. When dealing with DC systems, the design of the battery bank, for storage requires major attention. Lead batteries outperform other types of batteries in terms of sustainability. There is a well-established recycling system in place that functions profitably while adhering to all environmental standards [5]. The widespread use of lead-acid batteries is due to their low cost, minimal self-discharge, high rate discharge, deep cycling, reliability, and ease of manufacture [5,6]

Among the various performance parameters of the battery system, the State of Charge (SOC) of the battery gives details about the residual capacity of the battery. Various other mentionable parameters under consideration are current, voltage, impedance and Depth of Discharge (DOD) and State of Health (SOH). SOC is the ratio of the cell's available capacity to its maximum possible ability or the proportion

of the battery's total capacity still available for further discharge [7-9]. In Eq. (1), *Q(t)* indicates the remaining capacity, and Q_n indicates the battery's nominal capacity specified by the manufacturers.

$$SOC = \frac{Q(t)}{Qn} \quad (1)$$

The most mentionable SOC estimation methods followed in the industry are direct measurement, adaptive systems, and hybrid methods [8,10,11]. Direct measurement involves directly measuring the physical properties of a battery such as current, voltage, impedance. Direct approaches for estimating SOC may be divided into 3 categories: Coulomb counting, Open Circuit Voltage (OCV), and Electrochemical Impedance Spectroscopy (EIS) [12]. The coulomb counting technique, commonly known as the Ah technique, is based on integrating the battery's current over time to compute the battery's remaining capacity. Because of its ease of implementation, the Ah method is the most often used methodology for estimating the SOC of a battery. The calculated SOC has significant errors related to the accumulated inaccuracies in current measurement caused by noises and the inaccurate initial value of the battery's SOC [13,14]. However, it can be successful in applications where the battery can be fully discharged for the recalibration of capacity [12]. A modified coulomb counting method is used to increase the accuracy of coulomb counting by determining a corrected current [15]. Both of the above strategies are also referred to as the bookkeeping approach [13].

Open Circuit Voltage (OCV) requires inputs like 1) OCV test, for analyzing the changes of electronic energy in electrode materials and SOC is correlated 2) terminal voltage test where the terminal voltage and Electro-Motive Force (EMF) is correlated with the SOC [16]. The impedance track method combines both voltage correlation and current integration methods, providing the benefits of both, but must be compensated for both temperature and discharge current [17]. In the impedance method, battery impedance is taken as an input and is used for finding out the SOC of the battery. But it varies for different battery specifications [18]. Impedance spectroscopy is an estimation method in which the impedance of the battery is taken at different charging and discharging currents. Impedance models are run with these inputs and SOC is derived using the predetermined impedance values [19]. Impedance spectroscopy is a precise procedure, but it necessitates specialised equipment, making it a slightly complicated technique that is difficult to execute in real-world applications [14].

Adaptive systems methods are capable of learning, and they may change the battery model by decreasing the error, which is the difference between the simulated result and the actual measurement, to deliver an accurate SOC. Some of these methods are Artificial Neural Network (ANN), Fuzzy Logic, Support Vector Machine (SVM) [12]. In addition, numerous techniques combining the neural network and fuzzy logic algorithms have been developed [12]. The ANN-based SOC indicator forecasts the current SOC based on a battery's recent history of voltage, current, and temperature conditions. In the back propagation (BP) neural network, using the recent past of voltage, current and ambient battery temperature, the SOC value is predicted [20]. The Radial Basis Function (RBF) neural network is a helpful SOC estimation technique for systems with missing detail. It can be used in a given collection to evaluate the relationships between 1 important sequence and the other comparative ones [21,22]. The Fuzzy Logic method can recognise, represent, manipulate, interpret, and utilise data and information that are vague and lack certainty robust. It improves the accuracy and flexibility of SOC estimate in the presence of cell inconsistency [23]. It can be done online for SOC estimation, but it needs much memory in real-world application [24]. SVM is a modern statistical learning theory-based learning machine. It takes voltage, current, and temperature data as input to the model, gives SOC as output, uses non-linear mapping for data mapping in some areas, and applies the linear algorithm in the function space [25,26]. Adaptive systems methods are collectively known as Black-box model-based methods [14]. An exact battery model is not required for SOC estimation using these approaches. The system is modified by comparing the calculated result to the actual measurement and the feedback from the error. After multiple continual modifications, a perfect battery model with high precision for SOC estimate may be developed. The majority of adaptive system approaches for SOC estimation give accurate results and are commonly employed in electric vehicle applications, demanding precise estimation.

The model-based techniques compute the difference between the simulated and measured voltages (i.e., the system error) and feed it back into the battery model via the model gain to alter the estimated system states while also minimising the error. This closed-loop technology strives to be as precise as possible in calculating the battery's SOC and depends on the precision of the battery model developed. Self-correction, online calculation, and dynamic SOC estimation are just a few of the benefits of these approaches. Some model-based approaches that have been widely investigated for accurately estimating

the battery's SOC include the sliding mode observer, Moving Horizon Estimation (MHE), Proportional Integral Observer (PIO), Particle Filter (PF), Kalman filter and Luenberger observer. Kalman estimator is a state estimator which predicts the next state. Measurement and time updates are the steps involved in the Kalman filter [13,27]. The EKF is known to be effective in forecasting the dynamic behaviour of the system from numerical data. One of the primary measures for achieving the battery management systems applied to the next-gen electric cars is the Extended Kalman Filter (EKF) application to estimate the SOC [28].

Hybrid methods are a combination of 2 SOC estimation techniques used to obtain a more accurate value of SOC [12]. The approach under this category combines either Coulomb counting and EMF, or Coulomb counting and Kalman filter combination. In the coulomb counting and EMF combination method, the battery EMF is measured at equilibrium, and coulomb counting is done further. In the hybrid method involving Kalman filter and coulomb counting, Kalman filter is used to estimate the initial SOC of battery and this value is given to coulomb counting technique for the further estimation of SOC. In the case of a hybrid approach requiring a combination of the per-unit device and the EKF combination method, a battery model is configured, and the absolute parameter values in the equivalent circuit model are converted into dimensionless values in addition to the terminal voltage and current relative to the base value range [16]. Among the different techniques for SOC, the hybrid techniques are found to give a more accurate value of SOC. The proposed approach is a hybrid approach that combines the ease of calculation of the terminal voltage approach with the accuracy of the model-based technique. Temperature-dependent fluctuation of battery parameter is not considered and is evaluated for error since the test set, and point of application is the same and have a minimum temperature range.

The following is how the paper is structured. Section 2 shows why the suggested SOC estimate is necessary. The equivalent circuit model of a Lead-Acid battery is detailed. The battery characteristic study circuit testing platform for the current investigation is described in section 3. The testing platform contains settling, discontinuous discharge, and discontinuous charge tests for model derivation from actual trials. SOC estimation methodology with the assistance of an algorithm flow chart is presented in Section 4. Algorithm verification and outcome analysis was done in Section 5. The succeeding final section concludes the paper.

Materials and methods

Proposed state of charge estimation

48 V DC and 48 V ELVDC Distribution System-Guidelines, are standardised by BIS IS 16711: 2017, considering various aspects like safety, distribution losses, re-use of existing 230/110 V AC utility eco-system, local sourcing capability, and its recognition as a primary DC voltage according to IS 12360:1988/ IEC60038 [29]. Demand Response (DR) is described as deviations from typical use habits by end-use consumers in response to increases in energy price over time or to reward payments intended to encourage lower electricity use at periods of high price [30]. Demand Side Management (DSM) and DR for the systems incorporating energy storage requires SOC estimation for decision making [7,31]. Since the battery is always connected to the grid on an LVDC grid, which defines the system's voltage, the estimation of open-circuit voltage for the measured terminal voltage and current is needed to estimate SOC.

The purpose of this technique for SOC estimation is to have a reasonably accurate estimation with less computation time and skills. SOC estimation must be quick since other energy management algorithms also need to be integrated with DSM or any Home Energy Management Systems (HEMS).

Tropical regions are relatively warm-humid zones and is characterised by high rainfall and high humidity. The temperature range is relatively small over the year, and sunshine is quite intense and reasonably even during the day. In a warm and humid climate such as in Kerala, the variation in temperature and humidity is not as extreme as in other world regions. Contrary to other battery SOC estimations conducted, the difference is that the battery is kept open at ambient condition, and studies are done. Coulomb counting cannot be used since the system is not aware of its initial SOC. Since it is a stand-alone system and may be shut down in between, it can lose data, which results in estimation error. Open circuit voltage determination is also impossible since the battery needs to be online always according to the present LVDC architecture. Here for the SOC estimation, terminal voltage and current are measured, and the Thevenin model developed in a similar climatic condition is used. The accuracy of the obtained SOC is compared with the estimated value using coulomb counting. The higher the order of the battery equivalent model, the better the accuracy of the result. But considering the processor performance of this particular application, it is acceptable to choose a battery model of lesser order [12].

Hence, the Thevenin model is selected to analyse parameters for the lead-acid battery equivalent circuit model shown in **Figure 1**. In **Figure 1** R_d is the series internal resistance, R_p and C_p are the polarisation resistance and polarisation capacitance, respectively, where V_p is the polarisation voltage. The parallel resistance and capacitance reflect the dynamic battery characteristics, V_{oc} is the open-circuit voltage, and V_t is the battery terminal voltage, and $I(t)$ is the charging and discharging current of the battery. The electrical expression corresponding to this model is described by Eqs. (2) and (3);

$$V_t = V_{oc} - V_p - I(t)R_d \tag{2}$$

$$\frac{(V_{oc}-V_t)}{I(t)} = R_d + \frac{R_p}{1+R_pC\omega} \tag{3}$$

Since the battery is connected to a DC grid and steady-state current and voltage is only taken into consideration for SOC estimation, the relation becomes;

$$V_{oc} = V_t + I(t)(R_d + R_p) \tag{4}$$

With this calculated V_{oc} from the terminal voltage and current, SOC is estimated. Initially, there is no idea about the present state of charge; hence an average R_d, R_p value was taken to calculate the initial V_{oc}. From the next step, the estimated SOC from the obtained initial V_{oc} was taken for generating the R_d, R_p values for the next set of calculation. From the next step onwards, the estimated SOC of the previous condition helps to find the R_p, R_d value for computing the present V_{oc}.

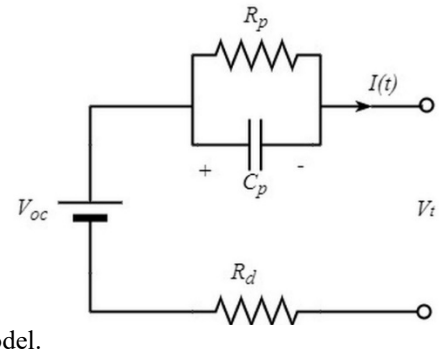

Figure 1 1st-order Thevenin model.

Battery characteristic study circuit

Different tests are performed on fully charged 4 series-connected 12 V, 7 Ah batteries to determine the battery model parameters. **Figure 2** shows the block diagram of the experimental setup for Thevenin model parameter determination and model verification.

Many tests are done to evaluate the batteries internal impedance value at different SOC states at different conditions such as charging, discharging and idle. First of all, the 4 batteries are connected in series to obtain 48 V system with 7 Ah capacity, and a loading rheostat is used as the load so the charging and discharging currents can be adjusted. Mainly 3 types of tests are done for finding the internal impedance values of the batteries. They are:

1) Settling test (To determine settling period)
2) Discontinuous discharge test (To determine battery model parameters at various SOC while discharging)
3) Discontinuous charge test (To determine battery model parameters at various SOC while charging)

Settling test

The settling test is carried out to determine the settling time of the battery for the discontinuous discharge and charge test. **Figure 3** shows the graph obtained after performing a discharge-settling test. From the graph, the settling time of the battery pack is derived as 2 h, which suggests that a time period of 2 h is needed for the battery pack to settle after a discharging cycle.

All the values for impedance parameters can be computed with the experimental method involving constant current discontinuous charging and discharging. In compliance with the voltage 0 state or 0 input response principle, the parameters in the circuit model are initialised. Ideally, the battery stays stagnant 2 h before each discharge in order to achieve the battery's V_{oc} open-circuit voltage. The DC discharge signal 1 A with a period of 21 min is then applied (mainly due to calibration efficiency) to obtain the remaining power at approximately 5 % SOC. Finally, the parameters corresponding to the remaining power values are inferred at intervals of 5 %. The 10 cycles of 5 % charging or discharging are done to obtain 50 to 100 % SOC and 100 to 50 % SOC, respectively. The experimental platform's battery monitoring device logs the shift of the battery terminal voltage along with the charging and discharging currents. **Figure 4** shows a typical discontinuous discharge cycle voltage profile

The reason for the sudden change of voltage after discharge is due to resistance R_d. During the discharge period it is known as R_{dd}. The voltage rises to 94 % of the final value after 3T time, which is because of R_p and C_p, otherwise known as the polarisation resistance and polarisation capacitance, respectively, denoted as R_{pd} and C_{pd} during discharge condition. Eqs. (5) - (7) shows the steps to compute R_{dd}, R_{pd}, C_{pd} for each cycle.

$$R_{dd} = \frac{\Delta V_1}{I} \tag{5}$$

$$R_{pd} = \frac{\Delta V_2}{I} \tag{6}$$

$$C_{pd} = \frac{T}{R_{pd}} \tag{7}$$

Discontinuous discharge test

Test procedure

This procedure involves charging the battery pack to 100 % SOC and settling for the first 2 h. The circuit is made ready and set to open circuit condition and run the program on the main controller. Next, the circuit is completed, and the discharge current is set to 1 A by adjusting the rheostat. This is followed by calibration of all the sensor calculations using the currently measured reference voltage. The program is again run on the main controller. The free serial monitor software is opened, and a text file is used for logging data which is later connected to the Arduino board, and then logging is initiated. After the test process, the logged data is subjected to excel sheet-based calculations and studies. Dynamic discharge test graph is plotted using the data logged, and the graph is shown in **Figure 5**. It shows the terminal voltage variation with respect to discontinuous current for the discontinuous discharge test. **Table 1** shows the obtained values for R_{dd}, R_{pd}, C_{pd} with respect to SOC variation between 0.68 - 0.96. An average value of R_{dd} = 1.03 Ω, Average of
R_{pd} = 1.41 Ω, is used initially for finding approximate SOC for further computation. **Figure 6** shows the relation between R_d and SOC during discharge condition. To obtain the empirical relation, 2nd-order and 3rd-order curve fitting were done and is given in Eqs. (8) and (9). With the 2nd order curve fitting itself, a better R^2 value was obtained. Hence, Eq. (8) could be used in the algorithm for SOC estimation.

Figure 7 shows the relation between *Rp* and SOC during discharge condition. The same curve fitting methods obtain the empirical relation Eqs. (10) and (11). With the 3rd-order curve fitting, a better R^2 value was obtained. Hence Eq. (11) could be used in the algorithm for SOC estimation.

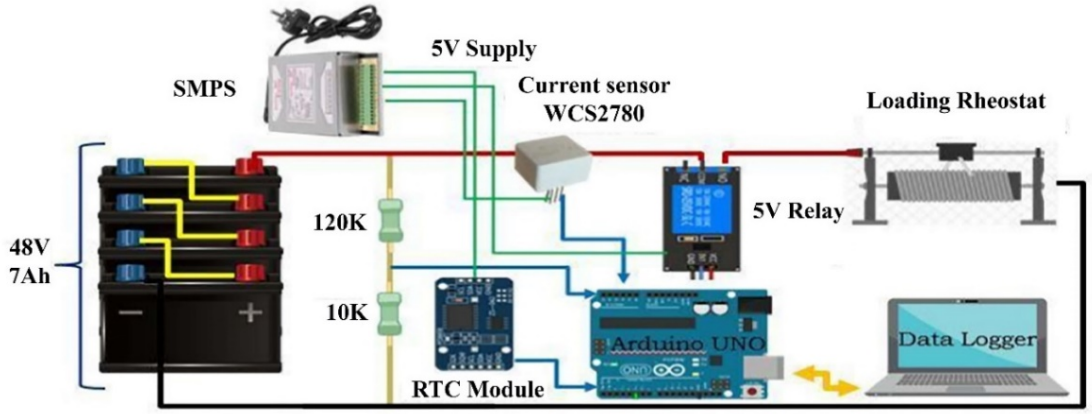

Figure 2 Discharge circuit for battery model determination and verification.

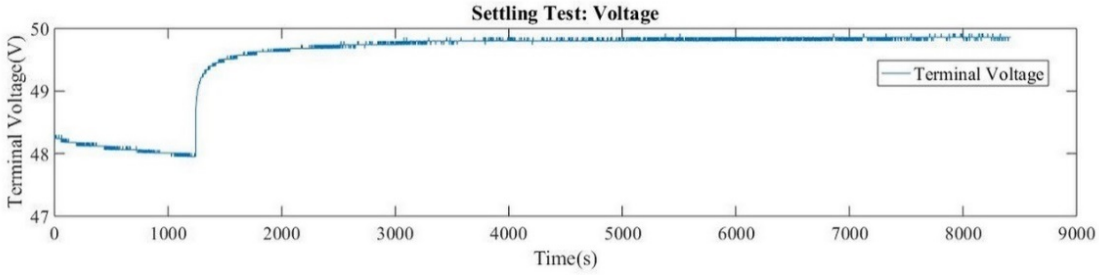

Figure 3 Settling test voltage profile.

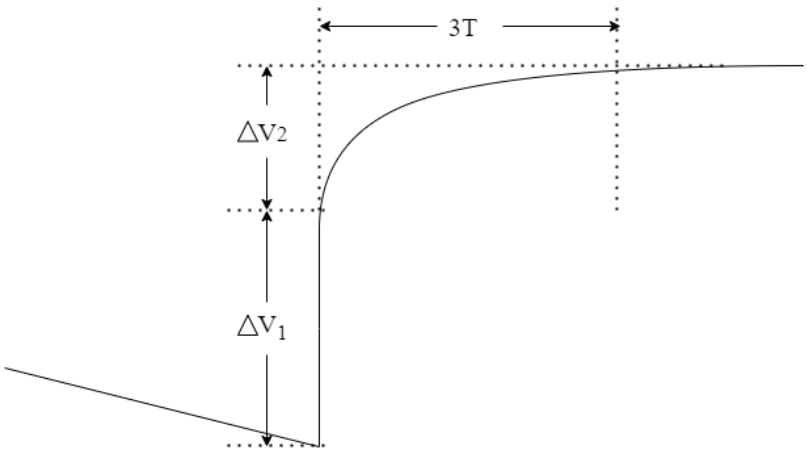

Figure 4 Discontinuous discharge cycle voltage profile.

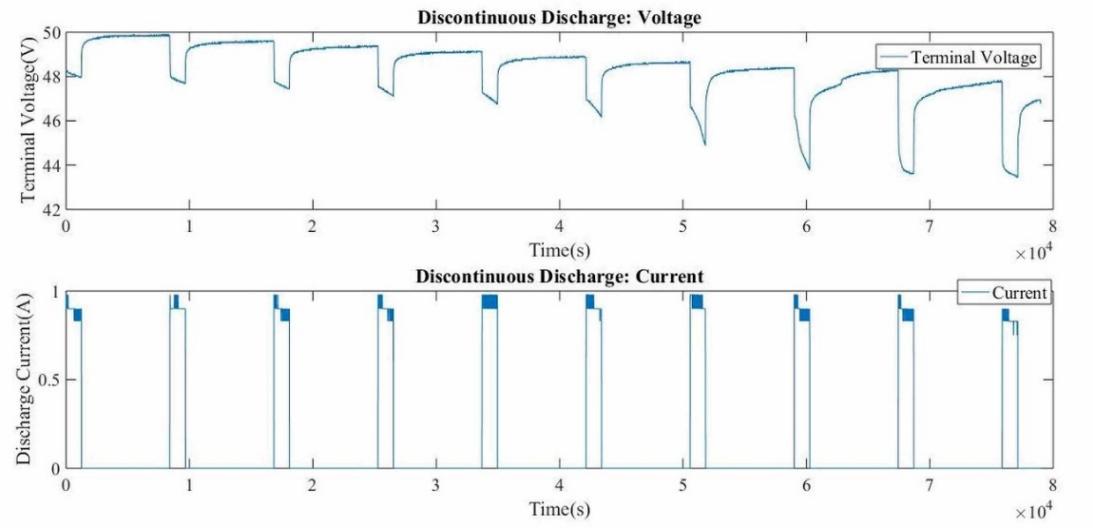

Figure 5 Discontinuous discharge test voltage and current.

Table 1 Calculated internal values from discontinuous discharge test.

V_t (V)	R_{dd} (Ω)	R_{pd} (Ω)	C_{Pd} (F)	SOC (0-1)
47.95	0.83	1.22	513.70	0.9555
47.66	0.83	1.22	632.67	0.9104
47.43	0.83	1.22	661.80	0.8654
47.14	0.92	1.25	607.96	0.82
46.73	1.02	1.26	681.61	0.7725
46.15	1.22	1.47	699.05	0.7266
44.88	1.54	2.20	313.21	0.6799

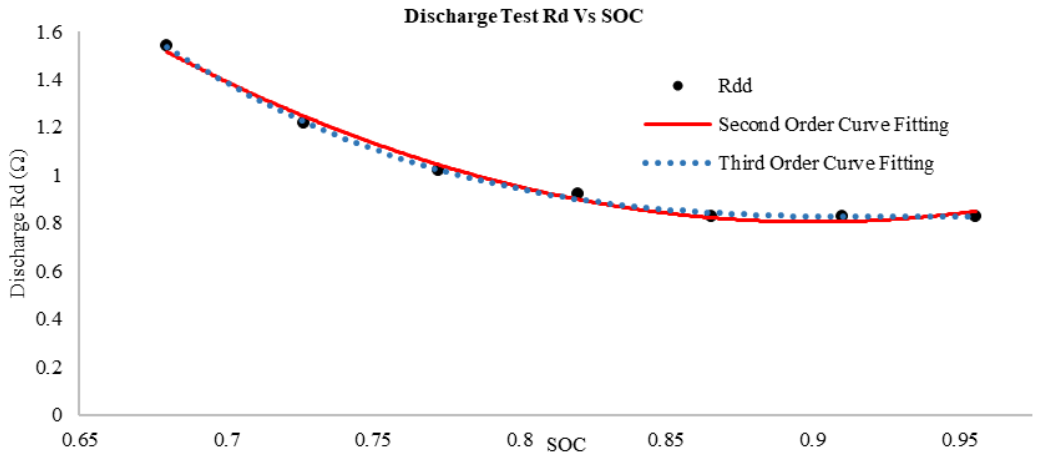

Figure 6 Discontinuous discharge test R_{dd} Vs SOC.

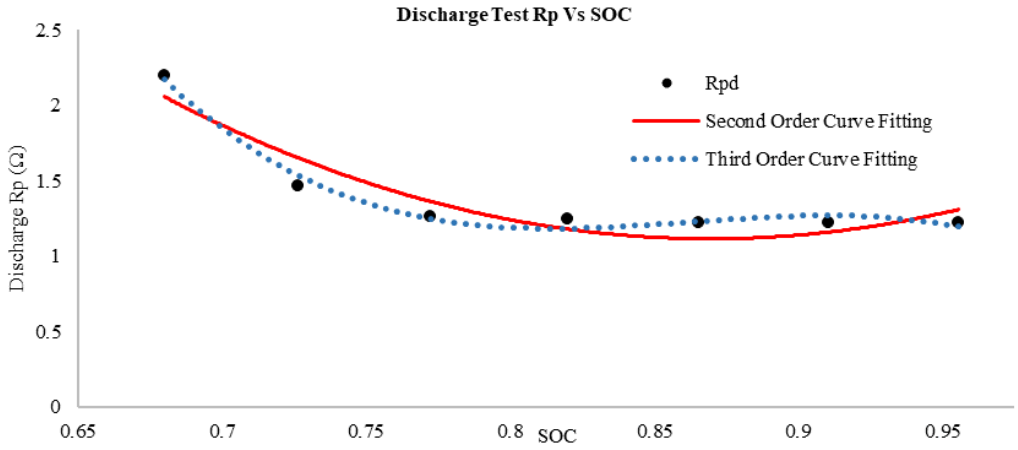

Figure 7 Discontinuous discharge test *Rpd* Vs SOC.

$$R_{dd} = 14.61\,SOC^2 - 26.31\,SOC + 12.65 \qquad R^2 = 0.9924 \tag{8}$$

$$R_{dd} = -35.95\,SOC^3 + 102.8\,SOC^2 - 97.91\,SOC + 31.88 \qquad R^2 = 0.9985 \tag{9}$$

$$R_{dd} = -35.95\,SOC^3 + 102.8\,SOC^2 - 97.91\,SOC + 31.88 \qquad R^2 = 0.9985 \tag{10}$$

$$R_{pd} = -195.8\,SOC^3 + 506.6\,SOC^2 - 435.5\,SOC + 125.7 \qquad R^2 = 0.9839 \tag{11}$$

Discontinuous charge test

Figure 8 shows the circuit diagram for the discontinuous charging test. **Figure 9** shows the voltage profile for a single cycle for the discontinuous discharge test. As discussed earlier, the reason of the sudden change of voltage after discontinuing charging is due to resistance R_d. During charging it is known as R_{dc}. Voltage settles to 94 % of its final value after 3T time. This is due to the factors R_{pc} and C_{pc} otherwise known as the polarisation resistance and polarisation capacitance during charging. **Figure 10** shows the discontinuous charge test result.

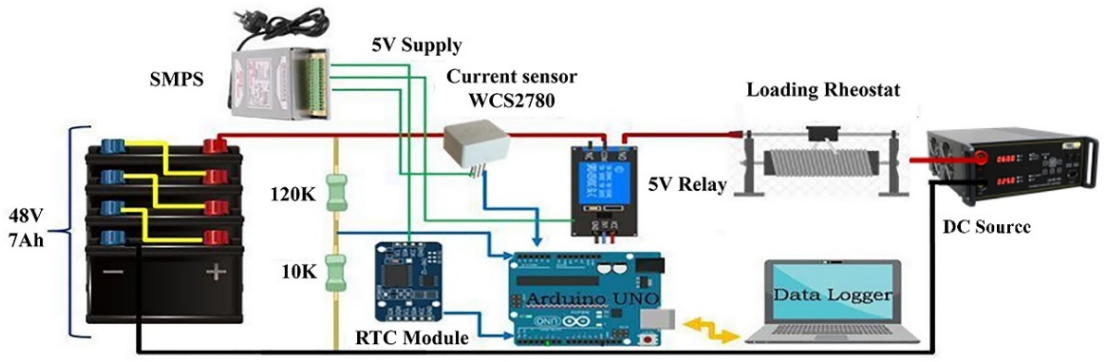

Figure 8 Charge circuit for battery model determination and verification.

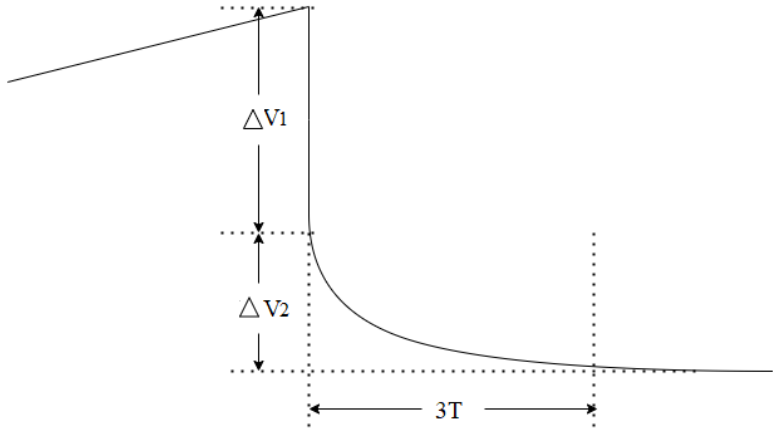

Figure 9 Discontinuous charge cycle voltage profile.

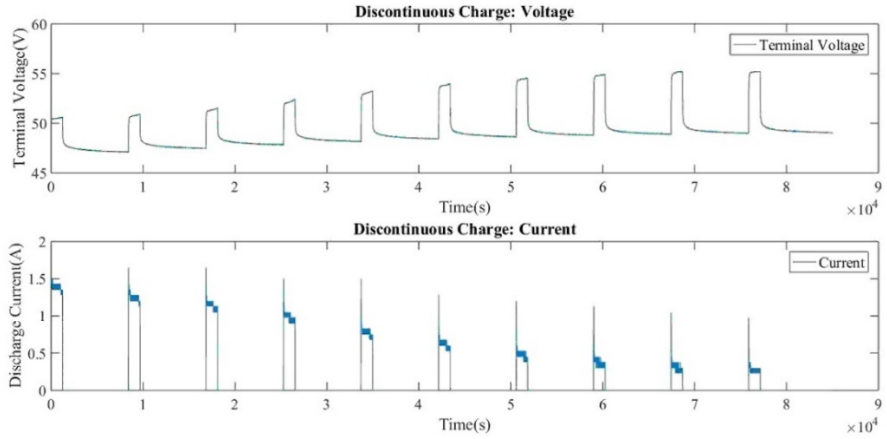

Figure 10 Discontinuous charge test voltage and current.

Table 2 shows the values obtained for SOC variation between 0.62 - 0.93. The values are obtained similar to discontinuous discharge test, for discontinuous charge test shown in **Figure 10**. Average values of R_{dc} = 4.31 Ω, and R_{pc} = 6.12 Ω, which will be used initially for finding approximate SOC for further computation.

Table 2 Calculated internal values from discontinuous charge test.

V_t (V)	R_{dc} (Ω)	R_{pc} (Ω)	C_{pc} (F)	SOC (0 - 1)
50.64	0.98	1.61	667.03	0.6172
50.92	1.01	1.85	492.82	0.6791
51.54	1.14	2.17	473.87	0.7358
52.38	1.81	2.715	386.07	0.7844
53.27	2.94	3.54	252.01	0.8245
53.95	4.41	4.67	239.99	0.8570
54.86	6.59	7.17	135.44	0.8811
54.84	7.24	9.31	82.75	0.8999
55.18	8.22	12.66	56.73	0.9153
55.18	8.73	15.50	50.42	0.9292

Figure 11 shows the relation between R_{dc} and SOC during charge condition. Inorder to obtain empirical relation 2nd order and 3rd-order curve fitting were done and shown in Eqs. (12) and (13). With 2nd order curve fitting itself, a better R^2 value was obtained. Hence Eq. (12) will be used in the algorithm for SOC estimation.

Figure 12 shows the relation between R_p and SOC during charge condition. Inorder to obtain empirical relation, 2nd order and 3rd-order curve fitting was done and given in Eqs. (14) and (15), With the 3rd-order curve fitting, a good R^2 value was obtained. Hence Eq. (15) will be used in the algorithm for SOC estimation.

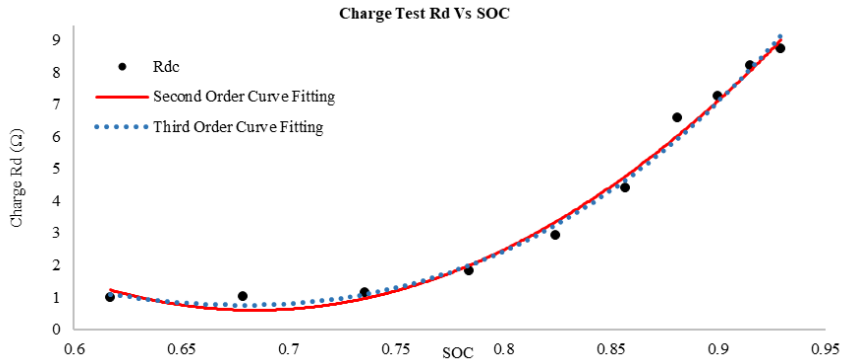

Figure 11 Discontinuous charge test R_{dc} Vs SOC.

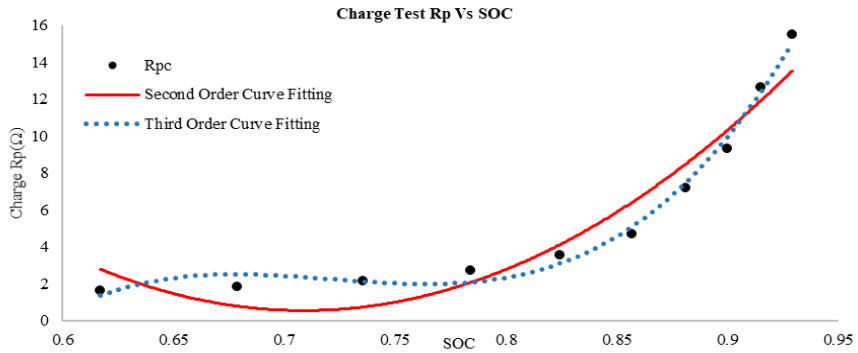

Figure 12 Discontinuous charge test Rpc Vs SOC.

$$R_{dc} = 140.1\,SOC^2 - 191.7\,SOC + 66.19 \quad R^2 = 0.9884 \tag{12}$$

$$R_{dc} = 150.2\,SOC^3 - 209.6\,SOC^2 - 76.73\,SOC - 1.758 \quad R^2 = 0.9897 \tag{13}$$

$$R_{pc} = 267.4\,SOC^2 - 379\,SOC + 134.9 \qquad R^2 = 0.9285 \tag{14}$$

$$R_{pc} = 1637\,SOC^3 - 3543\,SOC^2 + 2546\,SOC - 605.5 \qquad R^2 = 0.9907 \tag{15}$$

Figure 13 shows the relation between SOC and VOC. SOC is obtained by the coulomb counting method by charging the battery to full value and assuming the initial state as 100 %. The relation obtained, which is shown in Eq. 16 has an acceptable R^2 value. Increasing the order of curve fitting does not cause improvement in the R^2 values. Minor errors may be due to the slight variation in temperature during various SOC and the coulomb counting method. The accuracy of the developed method and model for estimating SOC can be checked by testing the battery with known SOC.

$$SOC = 0.1349\,VOC - 5.757 \qquad R^2 = 0.8717 \tag{16}$$

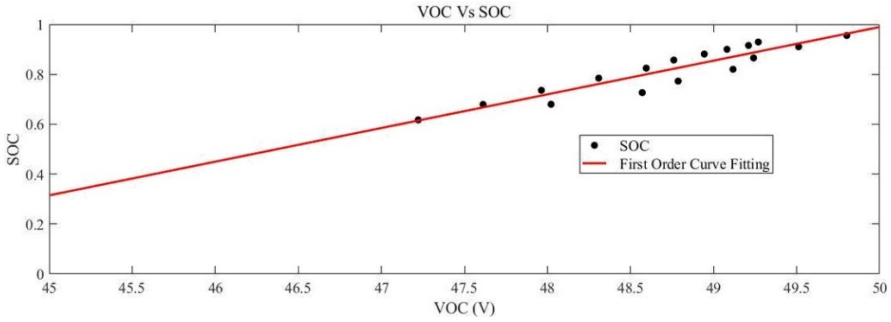

Figure 13 SOC Vs VOC.

Proposed SOC estimation algorithm

Terminal voltage and current of the battery is measured for SOC estimation. The direction of current measured determines the battery's charging or discharging condition. Accordingly, the internal resistance characteristics necessary to assess the open-circuit voltage are chosen and generated. The SOC is calculated using Eq. (16) and open-circuit voltage. An initial approximate SOC and present current direction is required to calculate the internal resistance parameter for estimating the SOC. Initially, the control circuit is unaware of the present SOC. Hence with the help of the average of internal resistance parameters, the initial SOC of the algorithm is estimated. **Figure 14** depicts the proposed SOC estimation method algorithm as a flow chart.

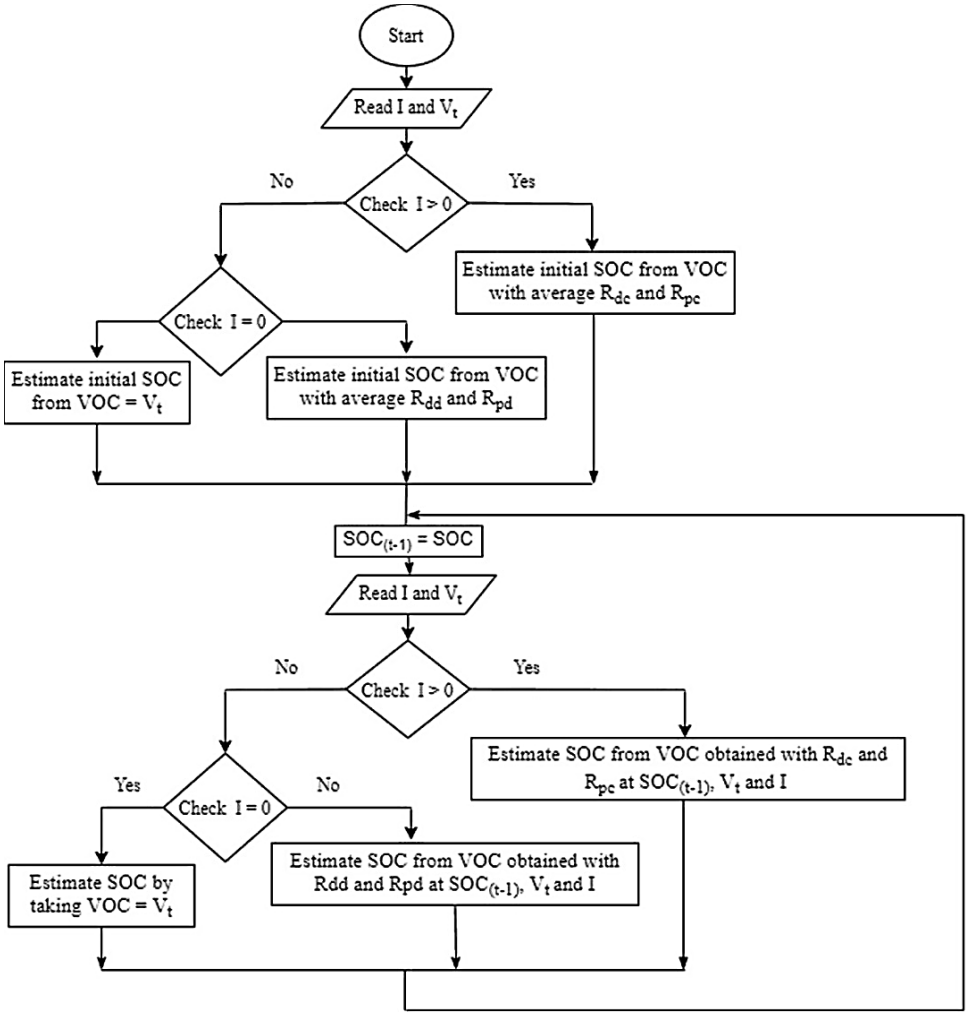

Figure 14 Proposed method flow chart.

Proposed SOC estimation method test result and discussions

The test setup was arranged at the exact location where the battery characterisation circuit was performed but at a different time. Temperature and humidity changes are minimal in Kerala, where these experiments were performed, due to its tropical climate. Compared to other battery SOC estimation method tests, the difference here is that the battery was kept open at room temperature while the trials were carried out. The proposed technique was tested and confirmed practically as the study is location-specific. To determine the accuracy of the devised approach, the SOC obtained was compared to the SOC obtained by coulomb counting. Based on the claim that the location's temperature change is insignificant, SOC estimation based on a temperature independent battery model was proposed. It should be verified at ambient conditions. Since coulomb counting SOC estimation is unaffected by temperature errors, comparing the proposed method to coulomb counting with an initial errorless value could reveal the percentage of error of the proposed method. The battery was initially fully charged to guarantee the accuracy of coulomb counting, and the initial SOC was set at 100 %.

Figure 15 shows the percentage error of the proposed method and a coulomb counting method set with a wrong initial value of 98 %; both compared with accurate SOC value using coulomb counting. It is observed that the percentage error in SOC estimation always falls under 2.5 %. The average error of SOC estimated using the proposed method is 0.71 %. This error may be attributed to error in the measurements of current or voltage and slight temperature variation. But for this specific application, which decides the conditions of operation based on a range of SOC values, this error is acceptable. When computed using coulomb counting, the average percentage error was 2.155 %, which again increases depending on the error in the initial state of charge and noise in current measurements. Processor requirements and time for estimation are lesser since the 1st-order battery model is used and no adaptive methods are involved in SOC estimation, which was proved in previous literature.

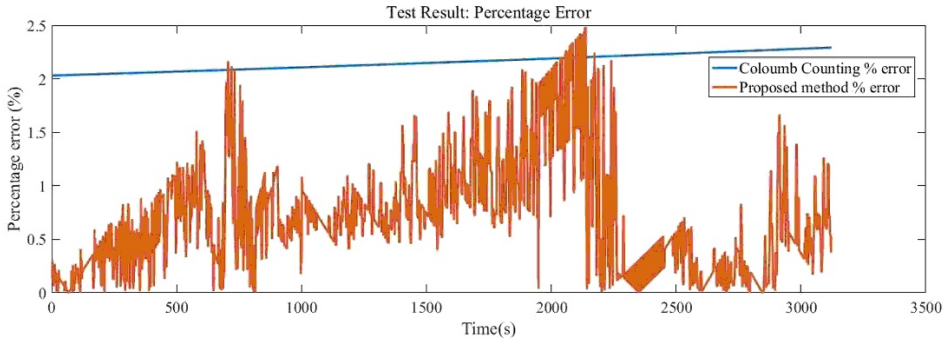

Figure 15 Test result error percentage.

Conclusions

Here a 48 V DC distribution with on-site solar power generation and a battery bank was considered. The principal purpose of the proposed project was to compile information that can guide and help overcome barriers to SOC estimation for DC power systems in buildings. An accurate method for the estimation of SOC for batteries makes the system more stable and also helps to reduce the battery sizing and improves battery life. Since LVDC architecture is a self-contained renewable energy system, any power interruption may cause data loss, leading to inaccurate coulomb counting estimates. Open circuit voltage determination is also impossible since the battery needs to be online always. Because the current is changing and terminal voltage relies on current values, SOC estimation using terminal voltage measurement never gives reliable results. In the proposed SOC method, the open-circuit voltage is estimated by measuring the terminal voltage, current and 1st-order model of the battery developed under similar climatic condition. It is proved that with the proposed system, a reasonably accurate SOC estimation of battery with lesser processor requirements can be achieved, especially for the tropical regions, where the temperature variations are negligible. Additionally, the proposed method brings the added advantage of being user friendly and closer to real-life situations as the measurements and modelling was done at the point of use. In future, the proposed method and coulomb counting can be implemented in the same system to observe the error for a whole year.

Acknowledgements

The work was supported by the project "APJ Abdul Kalam Technological University: Centre for Engineering Research and Development - Engineering Colleges Financial Assistance to Students" under the formal number: KTU/RESEARCH2/3895/2018 titled "Advanced DSM System for DC Residential Building."

References

[1] V Janamala. Solar PV tree: Shade-free design and cost analysis considering Indian scenario. *Walailak J. Sci. Tech.* 2021; **18**, 8995.
[2] D Groppi, A Pfeifer, DA Garcia, G Krajačić and N Duić. A review on energy storage and demand side management solutions in smart energy islands. *Renew. Sustain. Energ. Rev.* 2020; **135**, 110183.
[3] H Khorramdel, B Khorramdel and M Poshtyafteh. Programming of energy storage system in an island microgrid with photovoltaic and fuel cell. *Walailak J. Sci. Tech*. 2015; **12**, 361-71.
[4] International Electrotechnical Commission. *LVDC: Electricity for the 21st century*. International Electrotechnical Commission, Geneva, Switzerland, 2017.
[5] GJ May, A Davidson and B Monahov. Lead batteries for utility energy storage: A review. *J. Energ. Storage* 2018; **15**, 145-57.
[6] V Esfahanian, AA Shahbazi and F Torabi. A real-time battery engine simulation tool (BEST) based on lumped model and reduced-order modes: Application to lead-acid battery. *J. Energ. Storage* 2019; **24**, 100780.
[7] RK Chauhan, C Phurailatpam, BS Rajpurohit, FM Gonzalez-Longatt and SN Singh. Demand-side management system for autonomous DC microgrid for building. *Tech. Econ. Smart Grids Sustain. Energ.* 2017; **2**, 4.
[8] V Pop, HJ Bergveld, PHL Notten and PPL Regtien. State of the art of battery state of charge determination. *Meas. Sci. Tech.* 2005; **16**, R93.
[9] J Kim and BH Cho. Screening process-based modeling of the multi-cell battery string in series and parallel connections for high accuracy state-of-charge estimation. *Energy* 2013; **57**, 581-99.
[10] V Nandhini, K Bharathi, S Giri, S Sowvav and A Suyampulingam. Energy management and smart control of home appliances. *J. Phys. Conf. Ser.* 2020; **1706**, 012087.
[12] S Piller, M Perrin and A Jossen. Methods for state-of-charge determination and their applications. *J. Power Sourc.* 2001; **96**, 113-20.
[13] S Boulmrharj, R Ouladsine R, Y NaitMalek, M Bakhouya, K Zine-dine, M Khaidar and M Siniti. Online battery state-of-charge estimation methods in micro-grid systems. *J. Energ. Storage* 2020; **30**, 101518.
[14] CT Ma. Design and implementation of a hybrid real-time state of charge estimation scheme for battery energy storage systems. *Processes* 2020; **8**, 2.
[15] HS Ramadan, M Becherif and F Claude. Extended kalman filter for accurate state of charge estimation of lithium-based batteries: A comparative analysis. *Int. J. Hydrogen Energ*. 2017; **42**, 29033-46.
[16] K Soon, CS Moo, YP Chen and YC Hsieh. Enhanced coulomb counting method for estimating state-of-charge and state-of-health of lithium-ion batteries. *Appl. Energy*. 2009; **86**, 1506-11.
[17] W Chang. The state of charge estimating methods for battery: A review. *Int. Sch. Res. Not. Appl. Math.* 2013; **1**, 953792.
[18] K Petr. Methods of SoC determination of lead acid battery. *J. Energ. Storage* 2018; **15**, 191-5.
[19] AH Anbuky and PE Pascoe. VRLA battery state-of-charge estimation in telecommunication power systems. *IEEE Trans. Ind. Electron*. 2000; **47**, 565-73.
[20] K Bundy, M Karlsson, G Lindbergh and A Lundqvist. An electrochemical impedance spectroscopy method for prediction of the state of charge of a nickel-metal hydride battery at open circuit and during discharge. *J. Power Sources* 1998; **72**, 118-25.
[21] CW Zhang, SR Chen, HB Gao, KJ Xu and MY Yang. State of charge estimation of power battery using improved back propagation neural network. *Batteries* 2018; **4**, 69.
[22] J Chen, Q Ouyang, C Xu and H Su. Neural network-based state of charge observer design for lithium-ion batteries. *IEEE Trans. Contr. Syst. Tech*. 2018; **26**, 313-20.
[23] Y Guo, Z Yang, K Liu, Y Zhang and W Feng. A compact and optimized neural network approach for battery state-of-charge estimation of energy storage system. *Energy* 2021; **219**, 119529.
[24] L Hu, X Hu, Y Che, F Feng, X Lin and Z Zhang. Reliable state of charge estimation of battery packs using fuzzy adaptive federated filtering. *Appl. Energ.* 2020; **262**, 114569.

[25] D Saji, PS Babu and K Ilango. SoC estimation of lithium-ion battery using combined coulomb counting and fuzzy logic method. *In:* Proceedings of the 4th International Conference on Recent Trends in Electronics, Information, Communication & Technology, Bangalore, India. 2019, p. 948-52.

[26] V Chandran, CK Patil, A Karthick, D Ganeshaperumal, R Rahim and A Ghosh. State of charge estimation of lithium-ion battery for electric vehicles using machine learning algorithms. *World Electr. Veh. J*. 2021; **12**, 38.

[27] J Li, M Ye, S Jiao, D Shi and X Xu. *State estimation of lithium battery based on least squares support vector machine.* DEStech Transactions on Environment Energy and Earth Science. Lancaster PA, United States, 2019, p. 248-51.

[28] N Watrin, B Blunier and A Miraoui. Review of adaptive systems for lithium batteries state-of-charge and state-of-health estimation. *In:* Proceedings of the IEEE Transportation Electrification Conference and Expo, Dearborn, Michigan, United States. 2012, p. 1-6.

[29] RMS Santos, CLGDS Alves, ECT Macedo, JMM Villanueva, LV Hartmann and SYC Catunda. Lead acid battery soc estimation based on extended kalman filter method considering different temperature conditions. *In*: Proceedings of the IEEE International Instrumentation and Measurement Technology Conference, Turin, Italy. 2017, p. 1-6.

[30] Bureau of Indian Standards. *Guidelines for 48 V ELVDC distribution system - IS 16711*. Bureau of Indian Standards, Delhi, India, 2017.

[31] SK Korkua and K Thinsurat. A load prioritization model for a smart demand responsive energy management system in the residential sector. *Walailak J. Sci. Tech.* 2014; **11**, 7-18.

[32] RK Chauhan, BS Rajpurohit, FM Gonzalez-Longatt, SN Singh. Intelligent Energy Management System for PV-Battery-based Microgrids in Future DC Homes. *Int. J. Emerg. Electr. Power Syst* 2016; **17**, 339-50.